

This article was originally published in a journal published by Elsevier, and the attached copy is provided by Elsevier for the author's benefit and for the benefit of the author's institution, for non-commercial research and educational use including without limitation use in instruction at your institution, sending it to specific colleagues that you know, and providing a copy to your institution's administrator.

All other uses, reproduction and distribution, including without limitation commercial reprints, selling or licensing copies or access, or posting on open internet sites, your personal or institution's website or repository, are prohibited. For exceptions, permission may be sought for such use through Elsevier's permissions site at:

<http://www.elsevier.com/locate/permissionusematerial>

Structural distinctions of Fe_2O_3 – In_2O_3 composites obtained by various sol–gel procedures, and their gas-sensing features

Maria I. Ivanovskaya^{a,*}, Dzmitry A. Kotsikau^a, Antonietta Taurino^b, Pietro Siciliano^b

^a Research Institute for Physical Chemical Problems, Belarusian State University, 14 Leningradskaya, 220030 Minsk, Belarus

^b Institute of Microelectronics and Microsystems, IMM-CNR, Lecce Department, Via Arnesano, 73100 Lecce, Italy

Received 21 July 2006; received in revised form 5 December 2006; accepted 6 December 2006

Available online 8 January 2007

Abstract

New and various approaches to the sol–gel synthesis of advanced gas-sensing materials based on nanosized Fe_2O_3 – In_2O_3 (9:1 mol) mixed oxides, which differ in phase composition and grain size, have been considered in this paper. The correlation between the structural features of the composites and their gas-sensing behavior has been established. It was found that multi-phase Fe_2O_3 – In_2O_3 composites containing metastable γ - Fe_2O_3 structure are characterized by the greatest sensitivity to both reducing ($\text{C}_2\text{H}_5\text{OH}$) and oxidizing (NO_2) gases tested in this paper. The influence of synthesis conditions on the structural peculiarities of the Fe_2O_3 – In_2O_3 composites was studied in detail and the possibility to adjust fine structure of the materials was demonstrated.

© 2007 Elsevier B.V. All rights reserved.

Keywords: Fe_2O_3 – In_2O_3 nano-composites; $\text{C}_2\text{H}_5\text{OH}$ and NO_2 gas sensors; Structural characterization

1. Introduction

Composites based on iron and indium oxides are widely used as active layers of semiconducting gas sensors. The gas-sensing behavior of Fe_2O_3 – In_2O_3 -based sensors is essentially determined by the phase composition of the oxides, their dispersity and the Fe_2O_3 concentration [1–5].

A substantial literature on this topic has been published; Fe_2O_3 – In_2O_3 films containing γ - Fe_2O_3 modification of iron oxide are reported to be more sensitive to O_3 than α - Fe_2O_3 -based films [6]. Fe_2O_3 – In_2O_3 films with α - Fe_2O_3 as a main phase exhibit an enhanced response to $\text{C}_2\text{H}_5\text{OH}$ vapors as compared to In_2O_3 films slightly doped with Fe_2O_3 [1]. Chibirova and Gutman showed that the functional (in particular, gas-sensing) features of Fe_2O_3 -based oxides strongly depend on their pre-history, i.e. on the preparation procedure and mode of thermal treatment [7].

Nevertheless, a detailed structural distinction between the Fe_2O_3 – In_2O_3 films in relation to their dissimilar gas-sensing behavior has not been considered before.

In this paper, the structural peculiarities of Fe_2O_3 – In_2O_3 nanosized composites have been studied depending on the synthesis conditions and annealing temperature in order to assess the deposition parameters, which allow to obtain different structural modifications of Fe_2O_3 with different gas-sensing features.

The samples were obtained by inorganic modification of the sol–gel technology, which is based on the use of inorganic metal salts as precursors, as opposed to the classical modification using organic metal derivatives. The inorganic approach gives the possibility to prepare oxide composites in a nanosized state and to attain considerable mutual solubility of the components. It is worth noting that the used technology allows also to widely vary the phase composition and fine structure of the samples and therefore to control their gas-sensing characteristics.

2. Experimental

Fe_2O_3 – In_2O_3 samples with a Fe:In = 9:1 molar ratio and various phase composition were studied along with individual iron and indium oxides. The 9:1 molar ratio was found to be the most promising for gas-sensing applications [1].

The samples were synthesized as stabilized sols of the corresponding metal hydroxides. The synthesis procedures consisted of the following steps: (i) forced hydrolysis of an inorganic metal

* Corresponding author. Tel.: +375 172008106; fax: +375 172264696.

E-mail addresses: ivanovskaya@bsu.by (M.I. Ivanovskaya), pietro.siciliano@le.imm.cnr.it (P. Siciliano).

salt solution (0.5 mol l^{-1}) with a base agent (water solution of NH_3 , >99.99% purity, 0.5 mol l^{-1}); (ii) precipitation of a metal hydroxide and its separation from the liquid phase; (iii) formation of a sol by peptization of the deposit with peptizing agent (HNO_3) or as a result of self-peptization.

$\text{Fe}(\text{NO}_3)_3 \cdot 9\text{H}_2\text{O}$, FeSO_4 and $\text{In}(\text{NO}_3)_3 \cdot 4.5\text{H}_2\text{O}$ salts, all with stated purities >99.9%, were used as inorganic precursors for iron and indium oxides, respectively, both in simple and composite systems.

Single In_2O_3 and $\alpha\text{-Fe}_2\text{O}_3$ samples were synthesized by hydrolysis of $\text{In}(\text{III})$ and $\text{Fe}(\text{III})$ salts, respectively. The sols were obtained as a result of self-peptization of the corresponding metal hydroxides.

Single $\gamma\text{-Fe}_2\text{O}_3$ sol was obtained by oxidation of Fe_3O_4 sol at 100°C for 5 h by an intense flow of air. The sol of Fe_3O_4 was prepared by combined hydrolysis of $\text{Fe}(\text{III})$ and $\text{Fe}(\text{II})$ salts ($\text{Fe}(\text{III}):\text{Fe}(\text{II}) = 2:1 \text{ mol}$) with subsequent peptization.

The formation of $\text{Fe}_2\text{O}_3\text{-In}_2\text{O}_3$ sample based on $\alpha\text{-Fe}_2\text{O}_3$ ($\alpha\text{-Fe}_2\text{O}_3\text{-In}_2\text{O}_3$ sample) was achieved by combined hydrolysis of $\text{Fe}(\text{III})$ and $\text{In}(\text{III})$ salts.

$\text{I-}\gamma\text{-Fe}_2\text{O}_3\text{-In}_2\text{O}_3$ sample was prepared by simultaneous hydrolysis of $\text{In}(\text{III})$, $\text{Fe}(\text{III})$ and $\text{Fe}(\text{II})$ salts, and subsequent oxidation of the product.

An alternative way to obtain the $\text{Fe}_2\text{O}_3\text{-In}_2\text{O}_3$ system containing $\gamma\text{-Fe}_2\text{O}_3$ phase was attained by mixing the preliminary prepared individual In_2O_3 and $\gamma\text{-Fe}_2\text{O}_3$ sols ($\text{II-}\gamma\text{-Fe}_2\text{O}_3\text{-In}_2\text{O}_3$ sample).

Table 1 summarizes the synthesis conditions under which the above-mentioned oxides were obtained.

The structure of the samples was characterized by means of X-ray diffraction (XRD) analysis, high-resolution transmission electron microscopy (TEM), electron diffraction (ED), Mössbauer spectroscopy, and differential thermal analysis and thermogravimetry (DTA/TG). XRD analysis was carried out on a *HZG-4A* diffractometer by using $\text{Co K}\alpha$ radiation. TEM/ED examinations were performed with a *LEO 906E* and a *JEOL 4000 EX* high-resolution transmission electron microscopes. The resonance spectra were recorded in air at 298 K and processed by using a commercial SM2201 Mössbauer spectrometer

equipped with a $15 \text{ mCi } ^{57}\text{Co}$ (Rh) source. Simultaneous DTA and TG analyses were carried out on an *OD-102* instrument in air with a 5°C min^{-1} heating rate.

In order to obtain thin-film sensors, the sols were deposited by spin-coating onto special polycrystalline Al_2O_3 substrates ($3 \text{ mm} \times 3 \text{ mm} \times 0.25 \text{ mm}$) supplied with Pt interdigitated electrode structure on the front side and a Pt-heater on the rear side. The thickness of the thin films was estimated to be about 200 nm. The sensor elements were successively annealed at $300\text{--}400^\circ\text{C}$ for 96 h in air. A further thermal treatment up to $500\text{--}800^\circ\text{C}$ was performed in order to characterize the crystallization process of the $\text{Fe}_2\text{O}_3\text{-In}_2\text{O}_3$ composites. The gas-sensing responses of the films to $\text{C}_2\text{H}_5\text{OH}$ and NO_2 gases were studied and correlated with the structural properties of the active materials. Contact electric potential was applied to the interdigitated electrode structure and current through a sensing layer in air and in air–gas mixtures was measured. The response (*S*) of the sensors was calculated as $I_{\text{air}}/I_{\text{gas}}$ and $I_{\text{gas}}/I_{\text{air}}$ when detecting oxidizing (NO_2) and reducing ($\text{C}_2\text{H}_5\text{OH}$) gases, respectively. The measurements were performed in a flow chamber (0.2 l) at 0.3 l min^{-1} flow rate, 20°C temperature and 30% relative humidity.

3. Results and discussion

3.1. System $\alpha\text{-Fe}_2\text{O}_3\text{-In}_2\text{O}_3$

The $\alpha\text{-Fe}_2\text{O}_3\text{-In}_2\text{O}_3$ composite, obtained by combined hydrolysis of $\text{Fe}(\text{NO}_3)_3$ and $\text{In}(\text{NO}_3)_3$ salts and subsequent co-precipitation of the resulting $\text{Fe}(\text{III})$ and $\text{In}(\text{III})$ hydroxides, remains X-ray amorphous after its thermal treatment at $150\text{--}300^\circ\text{C}$ (Fig. 1). After annealing the composite at 500°C , broadened reflections of the $\alpha\text{-Fe}_2\text{O}_3$ phase (ref. JCPDS 33-0664) appear in the XRD pattern.

The increase of the experimental lattice parameters compared to the reference data for $\alpha\text{-Fe}_2\text{O}_3$ phase, as well as the absence of reflexes deriving from indium-oxide phases, can be explained by

Table 1
Synthesis conditions of the samples studied in the paper

Sample designation	Synthesis conditions
In_2O_3	Introduction of NH_3 solution into $\text{In}(\text{NO}_3)_3$ solution
$\gamma\text{-Fe}_2\text{O}_3$	Introduction of $\text{Fe}(\text{NO}_3)_3\text{-FeSO}_4$ (2:1 mol) solution into NH_3 solution and oxidation of the suspension with air (5 h, 100°C)
$\alpha\text{-Fe}_2\text{O}_3$	Introduction of NH_3 solution into $\text{Fe}(\text{NO}_3)_3$ solution
$\alpha\text{-Fe}_2\text{O}_3\text{-In}_2\text{O}_3$ (9:1)	Introduction of NH_3 solution into $\text{Fe}(\text{NO}_3)_3\text{-In}(\text{NO}_3)_3$ (9:1 mol) solution
$\text{I-}\gamma\text{-Fe}_2\text{O}_3\text{-In}_2\text{O}_3$ (9:1)	Introduction of $\text{Fe}(\text{NO}_3)_3\text{-FeSO}_4\text{-In}(\text{NO}_3)_3$ (9:4.5:0.75 mol) solution into NH_3 solution and oxidation of the suspension with air (5 h, 100°C)
$\text{II-}\gamma\text{-Fe}_2\text{O}_3\text{-In}_2\text{O}_3$ (9:1)	Mixing of $\gamma\text{-Fe}_2\text{O}_3$ and In_2O_3 (9:1 mol) sols

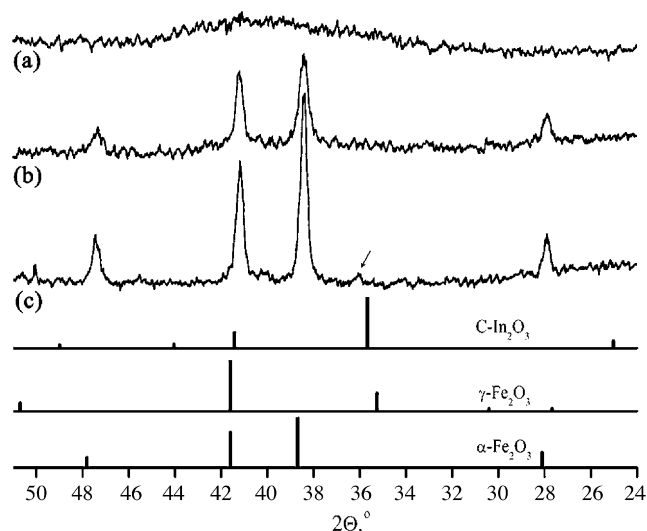


Fig. 1. XRD patterns of the $\alpha\text{-Fe}_2\text{O}_3\text{-In}_2\text{O}_3$ sample annealed at different temperatures: (a) 300°C ; (b) 500°C ; (c) 800°C .

Table 2

Comparison between the experimental interplanar spacings derived from the ED pattern in Fig. 2c and the theoretical values of the α -Fe₂O₃ phase

Line number	d_{measured} (Å)	α -Fe ₂ O ₃ (JCPDS 33-0664)		
		$d_{\text{calculated}}$ (Å)	I (%)	hkl
1	3.71	3.68	30	012
2	2.70	2.70	100	104
3	2.52	2.52	70	110
4	2.22	2.21	20	113
5	1.85	1.84	40	024
6	1.70	1.69	45	116
7	1.60	1.60	10	018
8	1.50	1.48	30	214
9	1.46	1.45	30	300

the formation of an α -Fe_{2-x}In_xO₃ solid solution, incorporating the total amount of indium within the α -Fe₂O₃ lattice. A high mutual solubility of α -Fe₂O₃ and In₂O₃ oxides at 600 °C has been reported in a previous work [5]. A noticeable destruction of the α -Fe_{2-x}In_xO₃ solid solution and isolation of individual C-In₂O₃ phase (*ref.* JCPDS 39-1346) start at 800 °C since its main diffraction reflection (marked with an arrow) can be distinguished in the corresponding XRD pattern. The shift of the reflection toward greater angle values (i.e. decrease of lattice parameters) is the evidence of substitution of indium ions by smaller iron ions in the In₂O₃ crystal lattice. A more detailed analysis of the fine structure of the α -Fe₂O₃-In₂O₃ composite annealed at 300 °C (not allowed by the XRD) was obtained by TEM/ED characterization. As shown by the images in Fig. 2a and b, the X-ray amorphous α -Fe₂O₃-In₂O₃ composite consists of small ($d \leq 10$ nm) near spherical grains. The ED pattern of this composite is reported in Fig. 2c.

The ED data presented in Table 2 demonstrate that α -Fe₂O₃ with hexagonal structure forms at the annealing temperature of 300 °C.

The Mössbauer spectrum of such a sample, reported in Fig. 3a, shows a paramagnetic doublet. The lack of a magnetic order ($B=0$) in the sample arises from its high dispersity. The occurrence of In³⁺ ions within the α -Fe₂O₃ crystalline lattice is likely to produce a distortion of the Fe³⁺ coordination environment symmetry and leads to an increased quadrupole splitting parameter (Δ), as compared to the value typical of the individual α -Fe₂O₃ oxide (Table 3) [8].

Table 3

Parameters of the ⁵⁷Fe Mössbauer spectra recorded from the Fe₂O₃-In₂O₃ composites and individual iron oxides annealed at 300 °C

Sample	δ (± 0.03 ; mm/s)	Δ (± 0.03 ; mm/s)	B (± 0.5 ; T)	W (± 5 ; %)	Phase
α -Fe ₂ O ₃ -In ₂ O ₃ (9:1) (Fe ³⁺ /In ³⁺ co-precipitation)	0.30	0.78	0	100	α -Fe _{2-x} In _x O ₃
I- γ -Fe ₂ O ₃ -In ₂ O ₃ (9:1) (Fe ³⁺ /Fe ²⁺ /In ³⁺ co-precipitation)	0.38	0.08	50.5	75	Q- γ -Fe ₂ O ₃
	0.53	0	0	15	C- γ -Fe ₂ O ₃
	0.22	0.69	0	10	α -Fe _{2-x} In _x O ₃
II- γ -Fe ₂ O ₃ -In ₂ O ₃ (9:1) (γ -Fe ₂ O ₃ /In ₂ O ₃ mixing)	0.33	0.02	48.5	100	γ -Fe ₂ O ₃
	0.34	-0.03	49.0	100	γ -Fe ₂ O ₃
	0.39	0.09	50.7	100	α -Fe ₂ O ₃
γ -Fe ₂ O ₃ (reference) [9]	0.34	-0.05	49.8	100	γ -Fe ₂ O ₃
α -Fe ₂ O ₃ (reference) [9]	0.38	0.12	51.5	100	α -Fe ₂ O ₃

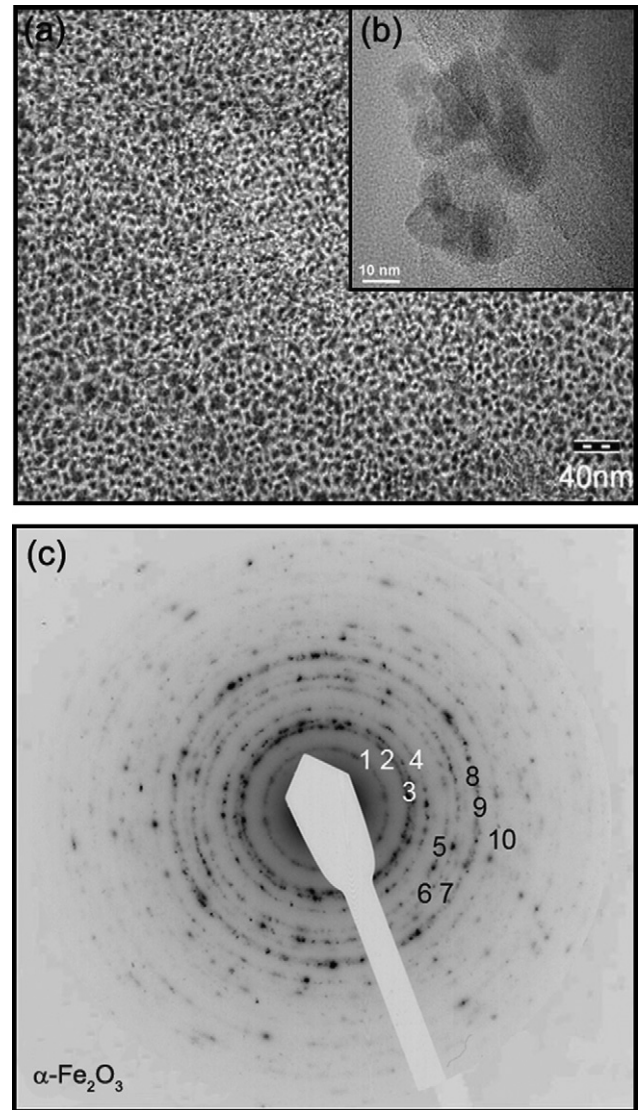


Fig. 2. TEM images (a and b) and ED pattern (c) of the α -Fe₂O₃-In₂O₃ sample annealed at 300 °C.

3.2. System γ -Fe₂O₃-In₂O₃

The formation of the γ -Fe₂O₃-In₂O₃ composite is related to the synthesis of the thermodynamically metastable γ -Fe₂O₃ phase. One of the approaches assumes the formation of γ -Fe₂O₃

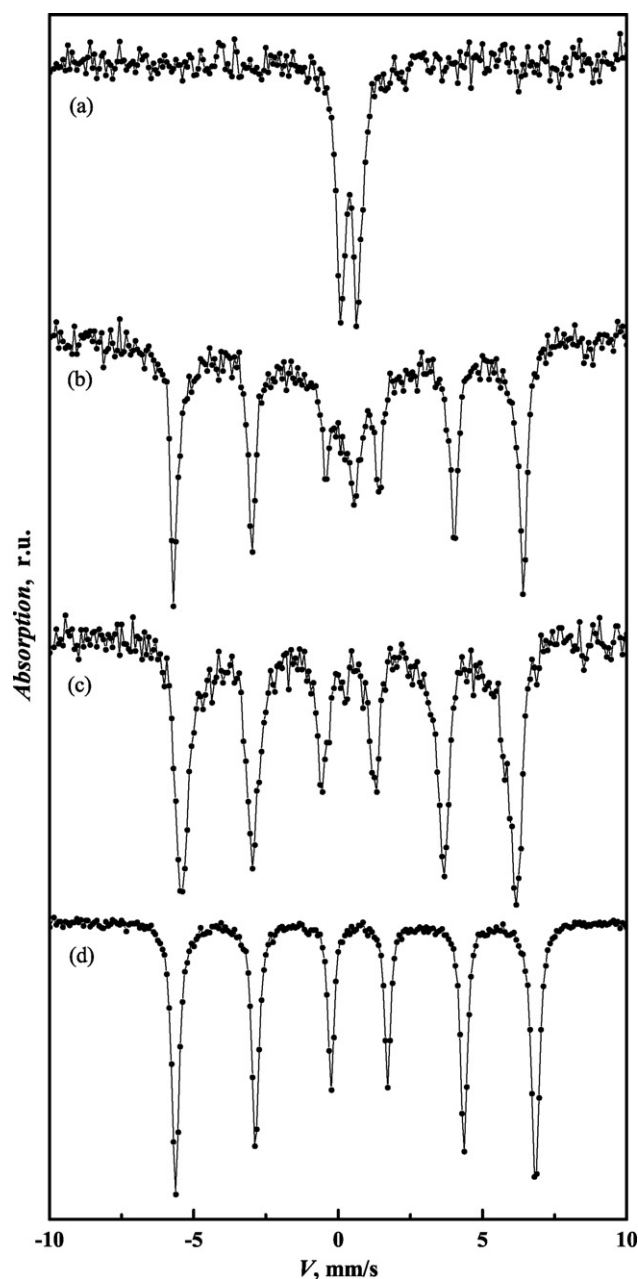


Fig. 3. ^{57}Fe Mössbauer spectra recorded from the samples annealed at 300 °C: (a) $\alpha\text{-Fe}_2\text{O}_3\text{-In}_2\text{O}_3$ (9:1); (b) $\text{I-}\gamma\text{-Fe}_2\text{O}_3\text{-In}_2\text{O}_3$ (9:1); (c) $\text{II-}\gamma\text{-Fe}_2\text{O}_3\text{-In}_2\text{O}_3$ (9:1); (d) $\alpha\text{-Fe}_2\text{O}_3$ (reference).

via magnetite (Fe_3O_4) intermediate. Magnetite has a structure, which is close to the structure of cubic $\gamma\text{-Fe}_2\text{O}_3$, differing from it in the absence of vacancies in the cationic sub-lattice. Thus, $\gamma\text{-Fe}_2\text{O}_3$ phase can be obtained by oxidation of Fe_3O_4 under controlled conditions [9,10].

The previous considerations allow to assume that the $\text{Fe}_2\text{O}_3\text{-In}_2\text{O}_3$ composite based on $\gamma\text{-Fe}_2\text{O}_3$ phase can be obtained by simultaneous hydrolysis of In(III) , Fe(III) and Fe(II) salts, and subsequent oxidation of the product. However, competitive processes, such as formation of $\alpha\text{-Fe}_2\text{O}_3$ and In_2O_3 phases, are possible under the indicated conditions. Moreover, the rates of hydrolysis of Fe(III) and Fe(II) salts are known to

Table 4

Comparison between the experimental interplanar spacings derived from the ED pattern in Fig. 5d and the theoretical values of the $\alpha\text{-Fe}_2\text{O}_3$ phase

Line number	d_{measured} (Å)	$\alpha\text{-Fe}_2\text{O}_3$ (JCPDS 33-0664)		
		$d_{\text{calculated}}$ (Å)	I (%)	hkl
1	2.71–2.53	2.70	100	104
		2.52	70	110
2	2.46–2.16	2.20	20	113
3	1.58–1.50	1.60	5	122
		1.60	10	018
		1.48	30	214
4	1.29–1.18	1.31	10	1010
		1.19	5	128

differ substantially [11,12]. Therefore, products of complicated phase composition can be expected [13].

The experimental X-ray data showed that the **I- $\gamma\text{-Fe}_2\text{O}_3\text{-In}_2\text{O}_3$** composite obtained under the above indicated synthesis conditions is amorphous for an annealing temperature of 150 °C. A crystalline structure appears after annealing at 300 °C, as visible in the relevant diffraction pattern reported in Fig. 4. It shows inhomogeneously broadened asymmetric reflections, which can be ascribed mainly to hexagonal $\alpha\text{-Fe}_2\text{O}_3$ phase, as well as, in minor measure, to both cubic (C- $\gamma\text{-Fe}_2\text{O}_3$) (ref. JCPDS 39-1346) and tetragonal (Q- $\gamma\text{-Fe}_2\text{O}_3$) (ref. JCPDS 25-1402, 13-0458) modifications of $\gamma\text{-Fe}_2\text{O}_3$.

This could be better evidenced by TEM and ED investigations, which confirmed the presence of anisotropic particles of Q- $\gamma\text{-Fe}_2\text{O}_3$ in the considered **I- $\gamma\text{-Fe}_2\text{O}_3\text{-In}_2\text{O}_3$** sample (Fig. 5). In particular, the sample is composed of two types of particles, which differ substantially in size and morphology. Fig. 5b shows highly dispersive ($d \sim 5$ nm) spherical grains whose ED pattern is typical of $\alpha\text{-Fe}_2\text{O}_3$ phase (Table 4). The second type of grains has a plate-like shape and a size of about 10 nm \times 30 nm. The analysis of the ED pattern obtained from such grains (Fig. 5e) reveals the presence of $\gamma\text{-Fe}_2\text{O}_3$ phase (Table 5); as the lattice parameters of C- $\gamma\text{-Fe}_2\text{O}_3$ ($a = 0.8340$ nm; symmetry group $Fd\bar{3}m$) and Q- $\gamma\text{-Fe}_2\text{O}_3$ ($a = 0.8338$ nm, $c/3 = 0.8322$ nm; symmetry group $P4_132$) are very similar, it is not possible to distinguish precisely between cubic and tetragonal modifications; nevertheless, the presence of both is expected, with a prevalence of the tetragonal one (ref. JCPD 25-1402), since the formation of the tetragonal $\gamma\text{-Fe}_2\text{O}_3$ phase is considered as perfecting the crystalline structure of C- $\gamma\text{-Fe}_2\text{O}_3$, during the annealing and crystal growth [10,14–16]. In particular, the degree of ordering of the cation vacancies increases, leading to the formation of a superstructure, peculiar to the tetragonal $\gamma\text{-Fe}_2\text{O}_3$ lattice cell but not to the cubic one (Fig. 6), where cation vacancies are distributed statistically between the octahedral interstices.

The electron diffraction gives also indications about the anisotropy of the Q- $\gamma\text{-Fe}_2\text{O}_3$ particles, as only high order l -index reflections appear (206, 119, 209, 316, 0012, 2112, 2015, 3315, 2224). These results are in agreement with the XRD data and confirm the anisotropic growth of the Q- $\gamma\text{-Fe}_2\text{O}_3$ crystals along the [001] orientation, which coincides with the

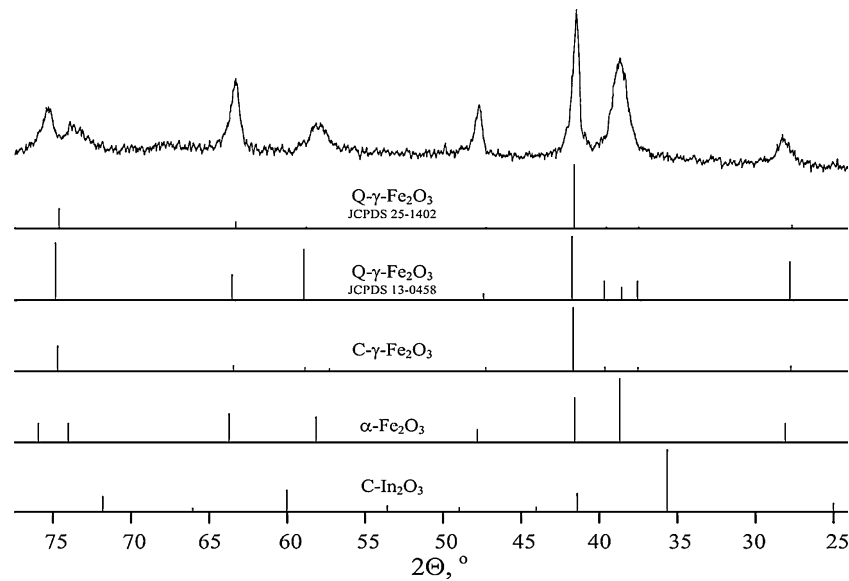


Fig. 4. XRD pattern of the **I- γ -Fe₂O₃-In₂O₃ (9:1)** composite annealed at 300 °C and stroke patterns of the reference phases.

vector of light magnetization in γ -Fe₂O₃ structure. The magnetic crystallographic anisotropy of γ -Fe₂O₃ favors both the anisotropic crystal growth and the formation of the tetragonal structure of γ -Fe₂O₃ lattice. No reflections due to any indium oxide phases were detected in the considered ED pattern. The absence of separate indium oxide phases in this sample was also confirmed by Mössbauer examination as described below.

An intricate Mössbauer spectrum of the **I- γ -Fe₂O₃-In₂O₃** sample (see Fig. 3b) reflects the complex phase composition of the oxide system obtained as a result of simultaneous hydrolysis of In(III), Fe(III) and Fe(II) salts. The results of the spectrum splitting (δ , Δ , B parameters) and phase compositions are listed

in Table 3 and allow to infer the following conclusions: most of the Fe³⁺ ions (~75%) have symmetry of coordination environment slightly different from cubic. This is typical of Q- γ -Fe₂O₃ structure. About 15% of the Fe³⁺ ions have parameters very close to those of C- γ -Fe₂O₃. Coordination symmetry of a minor part of the Fe³⁺ ions (~10%) differs substantially from cubic and can be the result of substitutional α -Fe_{2-x}In_xO₃ solid solution formation. The lack of magnetic ordering in the last two phases – C- γ -Fe₂O₃ and α -Fe_{2-x}In_xO₃ – is caused by the small size of the grains. No Fe²⁺ ions, which were initially introduced into the reaction media, were detected in the target product. These conclusions are in good agreement with the structural results of the TEM analysis.

Table 5

Comparison between the experimental interplanar spacings derived from the ED pattern in Fig. 5e and the theoretical values of the C- γ -Fe₂O₃ and Q- γ -Fe₂O₃ phases

Line number	d_{measured} (Å)	C- γ -Fe ₂ O ₃ (JCPDS 39-1346)			Q- γ -Fe ₂ O ₃ (JCPDS 25-1402)		
		$d_{\text{calculated}}$ (Å)	I (%)	hkl	$d_{\text{calculated}}$ (Å)	I (%)	hkl
1	2.99	2.95	35	2 2 0	2.95	30	2 0 6
2	2.46	2.52	100	3 1 1	2.51	100	1 1 9
1 ^a	2.33	2.32	1	3 2 0	2.32	2	2 0 9
2 ^a	2.24	2.23	1	3 2 1	2.23	2	3 1 6
3	2.12–2.05	2.09	16	4 0 0	2.09	15	0 0 12
4	1.83–1.79	1.82	2	4 2 1	1.82	3	2 1 12
3 ^a	1.56	1.55	1	5 2 0	1.55	2	2 0 15
5	1.51	1.48	34	4 4 0	1.52	3	2 1 15
4 ^a	1.40	1.39	1	4 4 2	–	–	–
6	1.28	–	–	–	1.27	8	3 3 15
5 ^a	1.23	1.23	1	6 3 1	–	–	–
6 ^a	1.15	1.14	1	7 2 1	–	–	–
7	1.09	1.09	7	7 3 1	1.09	10	2 1 21
8	1.05	1.04	3	8 0 0	1.04	7	0 0 24
7 ^a	0.97	^b	^b	^b	0.98	5	2 2 24
9	0.90	^b	^b	^b	^b	^b	^b
10	0.83	^b	^b	^b	^b	^b	^b
11	0.81	^b	^b	^b	^b	^b	^b

^a Spot reflection.

^b The data are absent.

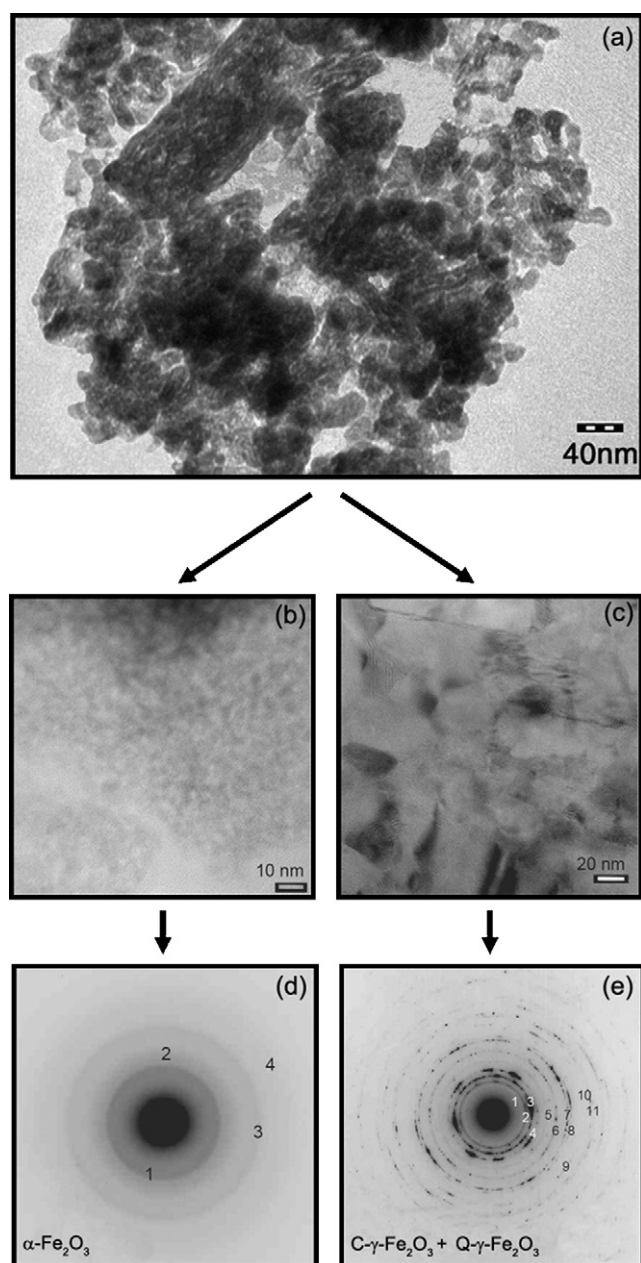


Fig. 5. TEM images (a–c) and ED patterns (d and e) of the **I- γ -Fe₂O₃-In₂O₃ (9:1)** sample annealed at 300 °C.

A TEM image of the **II- γ -Fe₂O₃-In₂O₃** sample, obtained by mixing the preliminary prepared individual **In₂O₃** and **γ -Fe₂O₃** sols and annealed at 300 °C, is given in Fig. 7. The sample consists of spherical grains with a diameter of 4–8 nm. XRD examination of the composite annealed at 150 °C shows the presence of the C- γ -Fe₂O₃ crystalline phase (Fig. 8). One weak (2 0 0)-reflection of InOOH phase is also present in the pattern. The increase of the annealing temperature to 300–400 °C causes the formation of the C- γ -Fe₂O₃ and C-In₂O₃ crystalline phases, whose experimental lattice parameters are in very good agreement with the reference data. According to DTA data, the thermo-stimulated γ -Fe₂O₃ → α -Fe₂O₃ transformation occurs in the considered **II- γ -Fe₂O₃-In₂O₃** composite at 455 °C that slightly exceeds the temperature of the same transformation in the individual **γ -Fe₂O₃** oxide (435 °C).

The obtained results give evidence that mixing individual sols of In₂O₃·*n*H₂O and γ -Fe₂O₃·*n*H₂O prevents oxide phases from mutual doping at the stage of their crystallization. The observed phenomenon can be connected with the specificity of the γ -Fe₂O₃·*n*H₂O sol synthesis. It includes a stage of long-term (5 h) oxidation of Fe₃O₄·*n*H₂O sol at rather high temperature (100 °C) that promotes both crystallization processes and particle growth. The lack of mutual doping in the considered composite was also confirmed by Mössbauer spectroscopy examination. Therefore, the spectrum parameters of the sample annealed at 300 °C are close to the parameters of the highly dispersed individual **γ -Fe₂O₃** sample (see Fig. 3; Table 3). However, the presence of indium in the **II- γ -Fe₂O₃-In₂O₃** composite influences grain size of the C- γ -Fe₂O₃ phase since the In₂O₃ grains seem to hamper the C- γ -Fe₂O₃ grain growth during the crystallization process.

Table 6 summarizes the results of various structural examinations of the **Fe₂O₃-In₂O₃ (9:1)** samples obtained under various synthesis conditions.

3.3. Gas-sensing features of the Fe₂O₃-In₂O₃ thin-film sensors

The thin-film sensors based on the obtained individual oxides (In₂O₃, α -Fe₂O₃, γ -Fe₂O₃), as well as on the Fe₂O₃-In₂O₃ composites with different structure, were tested to C₂H₅OH vapors and NO₂. Table 7 compares the maximum response values and optimal operating temperatures of the sensors. The corresponding signal profiles for the composites are given in Figs. 9 and 10. The α -Fe₂O₃-based sensor and especially

Table 6
Phase composition and grain size of the **Fe₂O₃-In₂O₃ (9:1)** samples studied in the paper

Composite	Synthesis conditions	Phase composition	<i>d</i> (nm)
I-α-Fe₂O₃-In₂O₃	Co-precipitation, Fe ³⁺ /In ³⁺	α -Fe _{2-<i>x</i>} In _{<i>x</i>} O ₃	3–10
I-γ-Fe₂O₃-In₂O₃	Co-precipitation, Fe ²⁺ /Fe ³⁺ /In ³⁺	α -Fe _{2-<i>x</i>} In _{<i>x</i>} O ₃	~5
		Q- γ -Fe ₂ O ₃	10 × 30
		C- γ -Fe ₂ O ₃	–
II-γ-Fe₂O₃-In₂O₃	Mixing, γ -Fe ₂ O ₃ /In ₂ O ₃	γ -Fe ₂ O ₃	4–8
		C-In ₂ O ₃	

Annealing temperature is 300 °C.

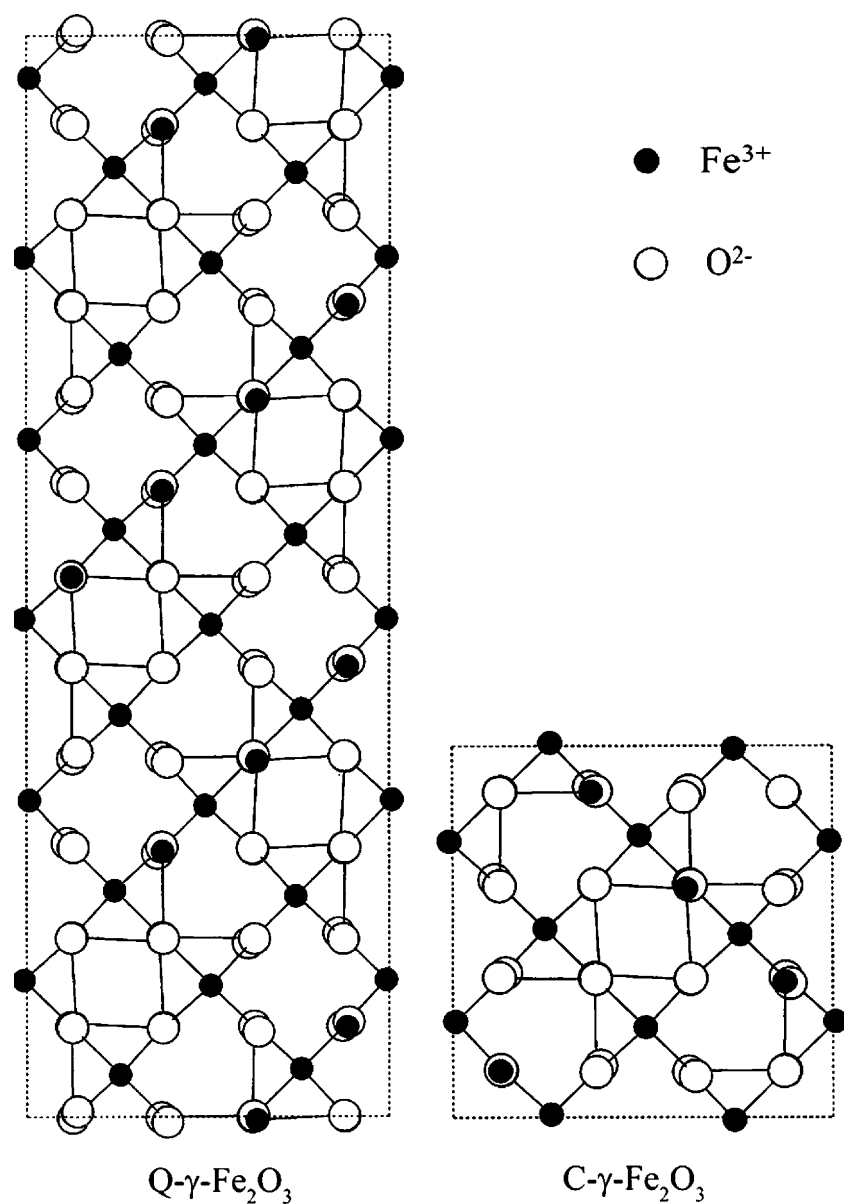
Fig. 6. Schematic representation of tetragonal (Q-) and cubic (C-) γ - Fe_2O_3 lattices, [0 1 0]-view.

Table 7

Phase composition of various oxide systems and gas-sensing features of the corresponding thin-film sensors regarding $\text{C}_2\text{H}_5\text{OH}$ vapors and NO_2

Sensing layer	Phase composition	$\text{C}_2\text{H}_5\text{OH}$ (50 ppm)		NO_2 (0.5 ppm)	
		S (r.u.)	t ($^{\circ}\text{C}$)	S (r.u.)	t ($^{\circ}\text{C}$)
α-Fe_2O_3-In_2O_3 (9:1)	α - $\text{Fe}_{2-x}\text{In}_x\text{O}_3$	2	250	1.5	135
I-γ-Fe_2O_3-In_2O_3 (9:1)	Q- γ - Fe_2O_3	27	250	75	135
	C- γ - Fe_2O_3				
	α - $\text{Fe}_{2-x}\text{In}_x\text{O}_3$				
II-γ-Fe_2O_3-In_2O_3 (9:1)	C- γ - Fe_2O_3	25	350	65	135
	C- In_2O_3				
In_2O_3	C- In_2O_3	15	350	35	150
α-Fe_2O_3	α - Fe_2O_3	9	250	1.5	200
γ-Fe_2O_3	γ - Fe_2O_3	15	300	5	200

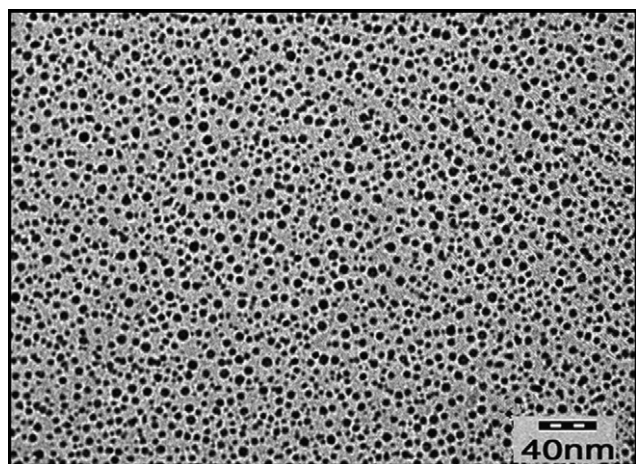


Fig. 7. TEM image of the **II- γ -Fe₂O₃-In₂O₃ (9:1)** sample annealed at 300 °C.

the **α -Fe₂O₃-In₂O₃** sensor show the lowest response values to both C₂H₅OH and NO₂. This result is expected since α -Fe₂O₃ phase is the most stable modification of iron oxide; therefore it should be less active in various electrophysical processes that cause a semiconductor sensor response. The poor performance of the **α -Fe₂O₃-In₂O₃** layer, which is formed of super fine particles of a single-phase α -Fe_{2-x}In_xO₃ solid solution, could be attributed both to its structural similarity to the α -Fe₂O₃-based sensor and to its extremely high resistance, which lower the sensitivity to the gas species [1].

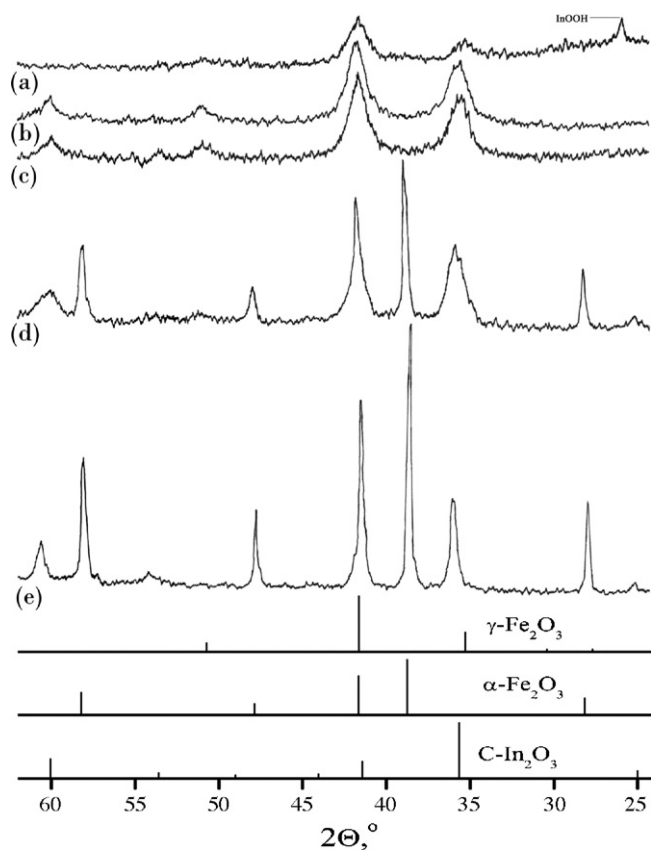


Fig. 8. XRD pattern of the **II- γ -Fe₂O₃-In₂O₃ (9:1)** composite annealed at different temperatures: (a) 150 °C; (b) 300 °C; (c) 400 °C; (d) 500 °C; (e) 800 °C.

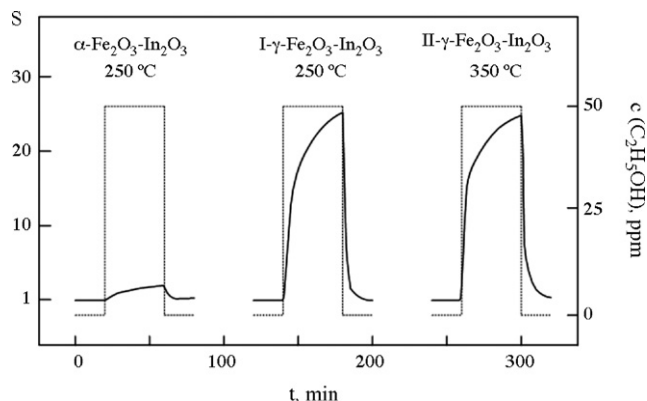


Fig. 9. Response curves of different **Fe₂O₃-In₂O₃** sensors to C₂H₅OH at optimal operating temperatures.

Individual **γ -Fe₂O₃** thin film, which is composed of γ -Fe₂O₃ phase, demonstrates higher response values to C₂H₅OH and NO₂ as compared to α -Fe₂O₃-based layers. The higher activity of the γ -Fe₂O₃ phase is associated with the specificity of its structure, its metastability, the presence of metal cation vacancies in crystalline lattice and the readiness of Fe²⁺ \leftrightarrow Fe³⁺ transformation upon exposure to gas media [4–7]. Besides, partial reversible reduction of a γ -Fe₂O₃-based material by C₂H₅OH to form α -Fe₂O₃ phase is possible. The product of reduction is highly dispersive and strongly reactive and resembles the behavior of γ -Fe₂O₃ [1,7].

The **II- γ -Fe₂O₃-In₂O₃** thin-film sensor exceeds the sensitivity of the sensors based on individual γ -Fe₂O₃ oxide. This is related to the presence in the **II- γ -Fe₂O₃-In₂O₃** composite of two highly dispersed phases: γ -Fe₂O₃ and In₂O₃. The heterojunction between these phases appears to be active in both adsorption and chemical transformation of C₂H₅OH and NO₂. The presence of two types of adsorption centers, having different reductive–oxidative and acid–base properties, and participating in the processes of the alcohol molecule transformation, is an essential requirement to achieve high sensor response when alcohol detection is considered. The centers of one type can suitably participate in adsorption–desorption processes of alcohol molecules, whereas complete oxidation effectively proceeds at

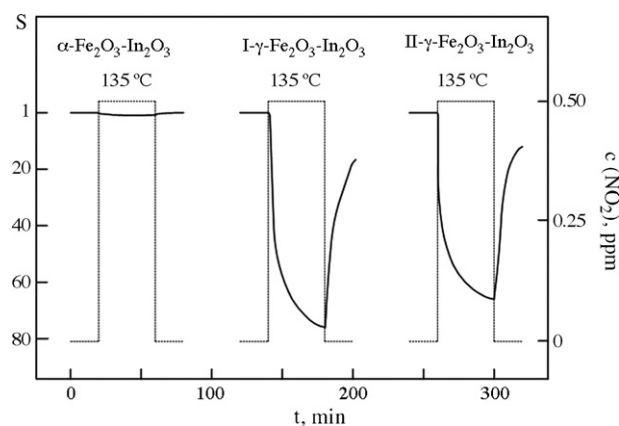


Fig. 10. Response curves of different **Fe₂O₃-In₂O₃** sensors to NO₂ at optimal operating temperatures.

the centers of the other type [1,17–19]. The most essential difference in sensitivity of the $\gamma\text{-Fe}_2\text{O}_3$ and $\text{II-}\gamma\text{-Fe}_2\text{O}_3\text{-In}_2\text{O}_3$ layers could be noted under detection of NO_2 . In the case of NO_2 detection, high defectiveness of oxide materials is the most critical requirement to achieve great response values [20].

As can be seen from the Table 7 and Figs. 9 and 10, the $\text{I-}\gamma\text{-Fe}_2\text{O}_3\text{-In}_2\text{O}_3$ sensor demonstrates the greatest sensitivity among the studied materials. As opposed to $\text{II-}\gamma\text{-Fe}_2\text{O}_3\text{-In}_2\text{O}_3$, this composite includes three phases: $\alpha\text{-Fe}_{2-x}\text{In}_x\text{O}_3$ solid solution, cubic $\gamma\text{-Fe}_2\text{O}_3$ and tetragonal $\gamma\text{-Fe}_2\text{O}_3$ with a superstructure of cationic vacancies. The developed interfacial areas between the indicated nanosized phases result in better sensing performance.

Both the $\text{I-}\gamma\text{-Fe}_2\text{O}_3\text{-In}_2\text{O}_3$ and $\text{II-}\gamma\text{-Fe}_2\text{O}_3\text{-In}_2\text{O}_3$ thin films excel substantially in sensitivity the sensors based on individual In_2O_3 and $\gamma\text{-Fe}_2\text{O}_3$ oxides, as well as earlier sensors based on $\text{In}_2\text{O}_3\text{-MoO}_3$ [20], $\text{In}_2\text{O}_3\text{-NiO}$ [21] and $\text{SnO}_2\text{-MoO}_3$ [22] composites. It is worth noting that in contrast to the individual $\gamma\text{-Fe}_2\text{O}_3$ layer, the $\text{II-}\gamma\text{-Fe}_2\text{O}_3\text{-In}_2\text{O}_3$ thin-film sensors appear to be more stable and selective to $\text{C}_2\text{H}_5\text{OH}$ vapors in the presence of CO , CH_4 , NO_2 and O_3 , as already demonstrated in [1].

Thus, high performances of the considered $\gamma\text{-Fe}_2\text{O}_3\text{-In}_2\text{O}_3$ gas-sensing layers were achieved by an optimal combination of grain size, surface activity, nature and amount of adsorption and catalytic centers. Moreover, the obtained results show that the more complex the structure of the $\text{Fe}_2\text{O}_3\text{-In}_2\text{O}_3$ composite the greater its response to gases of various chemical nature-oxidants (NO_2) and reductants ($\text{C}_2\text{H}_5\text{OH}$). As a matter of fact, the presence of adsorption centers of different nature on the surface of the complex $\text{Fe}_2\text{O}_3\text{-In}_2\text{O}_3$ gas-sensing materials creates the necessary prerequisites for multi-route activation of various reactions during the detection process.

4. Conclusion

The influence of synthesis conditions on the structural and gas-sensing properties of $\text{Fe}_2\text{O}_3\text{-In}_2\text{O}_3$ composites has been carefully analyzed. It was found that co-precipitation of Fe(III) and In(III) hydroxides leads to the formation of an $\alpha\text{-Fe}_{2-x}\text{In}_x\text{O}_3$ single-phase solid solution, which is homogeneous and poorly crystalline. The thermodynamic stability of this phase along with high structural homogeneity of the sample causes its poor sensitivity to both reducing and oxidizing gases.

The heterogeneous $\text{Fe}_2\text{O}_3\text{-In}_2\text{O}_3$ composite based on cubic In_2O_3 and metastable $\gamma\text{-Fe}_2\text{O}_3$ phases was obtained by mixing the individual sols of hydrated In_2O_3 and $\gamma\text{-Fe}_2\text{O}_3$ oxides. It demonstrates much greater response values due to high activity of metastable $\gamma\text{-Fe}_2\text{O}_3$ structure in adsorption and electrophysical processes.

Simultaneous precipitation of Fe(III) and Fe(II) hydroxides in the presence of In(III) salt results in a multi-phase product consisting of $\alpha\text{-Fe}_{2-x}\text{In}_x\text{O}_3$ solid solution, cubic $\gamma\text{-Fe}_2\text{O}_3$ and tetragonal $\gamma\text{-Fe}_2\text{O}_3$ phase with a superstructure of cationic vacancies. This structure provides substantial improvement of gas sensor performances in comparison with the homogeneous $\alpha\text{-Fe}_2\text{O}_3\text{-In}_2\text{O}_3$ composites. As general conclusion it can be

stated that the complexity of the oxide-based systems that appears as a stabilization of new phases and formation of structurally inhomogeneous nanosized heterojunction composites, gives new possibilities in the development of advanced gas sensors for detection of various gaseous species.

Acknowledgement

D. Kotsikau thanks the Belarusian Foundation of Fundamental Investigations for financial support.

References

- [1] M. Ivanovskaya, D. Kotsikau, G. Faglia, P. Nelli, S. Irkaev, Gas-sensitive properties of thin film heterostructures based on $\text{Fe}_2\text{O}_3\text{-In}_2\text{O}_3$ nanocomposites, *Sens. Actuators B: Chem.* 93 (2003) 422–430.
- [2] T. Takada, K. Suzuki, M. Nakane, Highly sensitive ozone sensor, *Sens. Actuators B: Chem.* 13 (1993) 404–407.
- [3] T. Takada, H. Tanjou, T. Saito, K. Harada, Aqueous ozone detector using In_2O_3 thin-film semiconductor gas sensor, *Sens. Actuators B: Chem.* 25 (1995) 548–551.
- [4] E.E. Gutman, Ozone sensor for the earth ozonosphere investigations, *Sens. Actuators B: Chem.* 25 (1996) 135–146.
- [5] M. Ristic, S. Popovich, M. Tonkovich, Chemical and structural properties of the system $\text{Fe}_2\text{O}_3\text{-In}_2\text{O}_3$, *J. Mater. Sci.* 26 (1991) 4225–4233.
- [6] E.E. Gutman, T.V. Belysheva, F.Kh. Chibirova, Structure effects in gas sensing by metal oxides, in: *Proc. XI Europ. Conf. on Solid-State Transducers (EUROSENSORS XI)*, vol. 1, Poland, Warsaw, 21–24 September, 1997, pp. 341–344.
- [7] F.Kh. Chibirova, E.E. Gutman, Structural defects and gas-sensing properties of some semiconducting metal oxides, *Russ. J. Phys. Chem.* 74 (9) (2000) 1555–1561.
- [8] V.I. Goldanski, *Chemical Application of Mössbauer Spectroscopy*, Mir, Moscow, 1980, pp. 167–177.
- [9] Y.S. Kang, S. Risbud, J.F. Rabolt, Synthesis and characterization of nanometer-size Fe_3O_4 and $\gamma\text{-Fe}_2\text{O}_3$ particles, *Chem. Mater.* 8 (1996) 2209–2211.
- [10] G.N. Kryukova, A.N. Shmakov, S.V. Tsybulya, A.L. Chuvilin, L.P. Solovyeva, V.A. Sadykov, Vacancy ordering in $\gamma\text{-Fe}_2\text{O}_3$: synchrotron X-ray powder diffraction and high-resolution electron microscopy studies, *J. Solid State Chem.* 89 (1990) 208–211.
- [11] F. Xu, X. Zhang, Y. Xie, Morphology control of $\gamma\text{-Fe}_2\text{O}_3$ nanocrystals via PEG polymer and accounts of its Mössbauer study, *J. Colloid Interface Sci.* 260 (1) (2003) 160–165.
- [12] R.M. Cornell, R. Giovanoli, W. Shneider, Review of the hydrolysis of iron(III) and the crystallization of amorphous iron(III) hydroxide hydrate, *J. Chem. Technol.* 46 (1989) 115–134.
- [13] A. Mandelis, C. Christofides, *Physics, Chemistry and Technology of Solid State Gas Sensor Devices*, John Wiley & Sons, New York, 1993, pp. 118–146.
- [14] T. Belin, N. Guigue-Millot, J.P. Bellat, J.C. Niepce, Influence of grain size, oxygen stoichiometry, and synthesis conditions on the $\gamma\text{-Fe}_2\text{O}_3$ vacancies Fe_2O_3 and lattice parameters, *J. Solid State Chem.* 163 (2002) 459–465.
- [15] G. Ennas, G. Marongui, A. Musinu, A. Falqui, P. Ballirano, R. Caminiti, Characterization of nanocrystalline $\gamma\text{-Fe}_2\text{O}_3$ prepared by wet chemical method, *J. Mater. Res.* 14 (4) (1999) 1570–1575.
- [16] M. Ivanovskaya, D. Kotsikau, G. Faglia, P. Nelli, Influence of chemical composition and structural factors of $\text{Fe}_2\text{O}_3/\text{In}_2\text{O}_3$ sensors on their selectivity and sensitivity to ethanol, *Sens. Actuators B: Chem.* 96 (2003) 498–503.
- [17] N. Yamazoe, New approaches for improving semiconductor gas sensors, *Sens. Actuators B: Chem.* 5 (1991) 7–19.
- [18] O.V. Krylov, *The Catalysis by Non-metals. The Appropriateness of the Catalysts Selection*, Khimia, Leningrad, 1967, pp. 98–117.

- [19] G.I. Golodets, Reductive–oxidative and acid–base steps of heterogeneous catalytic oxidizing reaction, catalysis mechanism, part 1, Nauka, Novosibirsk, 1984, pp. 142–158.
- [20] A. Gurlo, N. Barsan, M. Ivanovskaya, U. Weimar, W. Göpel, In_2O_3 and $\text{In}_2\text{O}_3\text{--MoO}_3$ thin film semiconductor sensors: interaction with NO_2 and O_3 , *Sens. Actuators B: Chem.* 47 (1998) 92–99.
- [21] M. Ivanovskaya, P. Bogdanov, G. Faglia, G. Sberverglieri, The features of thin film and ceramic sensors for the detection of CO and NO_2 , *Sens. Actuators B: Chem.* 68 (2000) 344–350.
- [22] M. Ivanovskaya, P. Bogdanov, G. Faglia, P. Nelli, G. Sberverglieri, On the role of catalytic additives in gas-sensitivity of SnO_2 -based thin film sensors, *Sens. Actuators B: Chem.* 70 (2001) 268–274.

Biographies

Dr. Maria I. Ivanovskaya received her degree in chemistry in 1980 from the Belarusian State University in the field of photochemistry. Since 1989 she has been working at the Research Institute for Physical Chemical Problems of the Belarusian State University. Her main scientific interest is solid state chemistry in applications to catalysis and semiconductor gas sensors, structural features of nanosized oxides (SnO_2 , MoO_3 , In_2O_3 , Fe_2O_3 , CeO_2 , ZrO_2 , La_2O_3) and oxide composites.

Dr. Dzmitry A. Kotsikau received his degree in chemistry in 2005 from Belarusian State University in the field of semiconductor gas sensors. Now he is working at the Research Institute for Physical Chemical Problems of the Belarusian State University in the field of semiconductor gas sensors and catalysts. His main scientific interests are $\text{Fe}_2\text{O}_3\text{--In}_2\text{O}_3$ and $\text{Fe}_2\text{O}_3\text{--SnO}_2$ nanosized composites, their structural and gas-sensitive characterization.

Dr. Antonietta Taurino took her PhD in physics in 1999 at the University of Lecce. Since 2001 she has been working as researcher at the Institute for Microelectronics and Microsystems of CNR. Her competences are related to the analysis of the morphological, structural and compositional properties of materials by transmission electron microscopy techniques, scanning transmission electron microscopy (STEM), electron beam induced current (EBIC), as well as by new techniques for nano-manipulation of materials by FIB. The main fields of interest are nanostructured thin films of single and mixed metal-oxides for gas sensors and III–V low dimensional semiconductors for optoelectronics.

Dr. Pietro Siciliano received his degree in physics in 1985 from the University of Lecce. He took his PhD in physics in 1989 at the University of Bari. During the first years of activities he was involved in research in the field of electrical characterization of semiconductor devices. He is currently working in the field of preparation and characterization of thin film for gas sensor and multisensing systems.